Preliminary mineralogical and analytical information on the gold bearing quartz-hematite vein of Mäkärä, Tana Belt, Northern Finland

Tegist Chernet, Yann Lahaye, Lassi Pakkanen, Olli Sarapää

February, 2018

GTK
gtk.fi

GEOLOGIAN TUTKIMUSKESKUS

Tekijät Tegist Chernet, Yann Lahaye, Lassi Pakkanen, Olli Sarapää	Raportin laji Arkistoraportti
	Toimeksiantaja Olli Sarapää

Raportin nimi
Preliminary mineralogical and analytical information on the gold bearing quartz-hematite vein of Mäkärä, Tana Belt, Northern Finland

Tiivistelmä

Mäkärä's gold and REE bearing quartz-hematite vein is studied by light and electron microscopes using polished sections from hard rock and non-magnetic heavy mineral concentrates of fragmented samples. The rock forming minerals are dominated by muscovite-sericite-chlorite associated with quartz, altered feldspar, hematite with minor amount of sulfides and Fe-Ti minerals. Important heavy minerals observed are gold, disseminated to aggregated grains of zircon, REE bearing minerals (Ce-variety monazite and Y-xenotime).

Gold assay results from drill core shows up to 7,96ppm, and the corresponding fine fraction (slime) up to 20ppm. Fine grained gold from heavy mineral concentrates display spongy or coral reef like to skeletal or dendritic structures. The composition indicates rather pure gold with trace amount of Ag and Fe. Monazite is the most common heavy mineral next to hematite and is often associated with rutile while xenotime is commonly associated with hematite.

The age of the Mäkärä gold bearing vein is estimated using in situ U-Pb geochronological analysis of zircon, monazite and xenotime on thin-sections. Zircons are rare and define several age populations. The youngest zircons have an age within error of the ages defined by monazite (1814 ± 21Ma) and xenotime (1781 ± 17), which corresponds well with the age of postorogenic granites.

Asiasanat (kohde, menetelmät jne.)
Gold, Mäkärä, Rare earth elements, Mineralogy, Geochronology, Northern Finland

Maantieteellinen alue (maa, lääni, kunta, kylä, esiintymä)
Finland, Lapland, Vuotso, Mäkärova, Mäkärä Au-rare earth element prospect

Karttalehdet V4343

Muut tiedot

Arkistosarjan nimi Archive series		Arkistotunnus 80/2017	
Kokonaissivumäärä 21	Kieli English	Hinta	Julkisuus
Yksikkö ja vastuualue Mineral Processing and Materials Research (MMA)		Hanketunnus 50408-80011	
Allekirjoitus/nimen selvennys Tegist Chernet		Allekirjoitus/nimen selvennys	

1   INTRODUCTION

The Mäkärä Au-rare earth element (REE) prospect area is located in the Tana Belt, south of the 1.9 Ga Lapland Granulite Belt, in northern Finland (Fig. 1). The Belt is composed of highly metamorphosed amphibolites, garnet-biotite and arkose gneisses and has prominent lanthanum (La) and yttrium (Y) anomalies in regional till and bedrock geochemical data (Sarapää and Sarala, 2014). At Mäkärä, promising narrow Au-hematite-quartz veins occur in connection with tensional fractures in the great shear zone (Härkönen 1987). In the shear zone chemical weathering has been intense causing kaolinization. The samples for this study was selected from the drill core R318, which penetrate Mäkärä gold-hematite-quartz-rock (Fig. 1). Drill core R318 intersects arkose gneiss, which around gold-bearing hematite has been altered to sericite-quartz rock or so-called Mäkärä quartzite. Arkose gneiss is characterized by lamination.
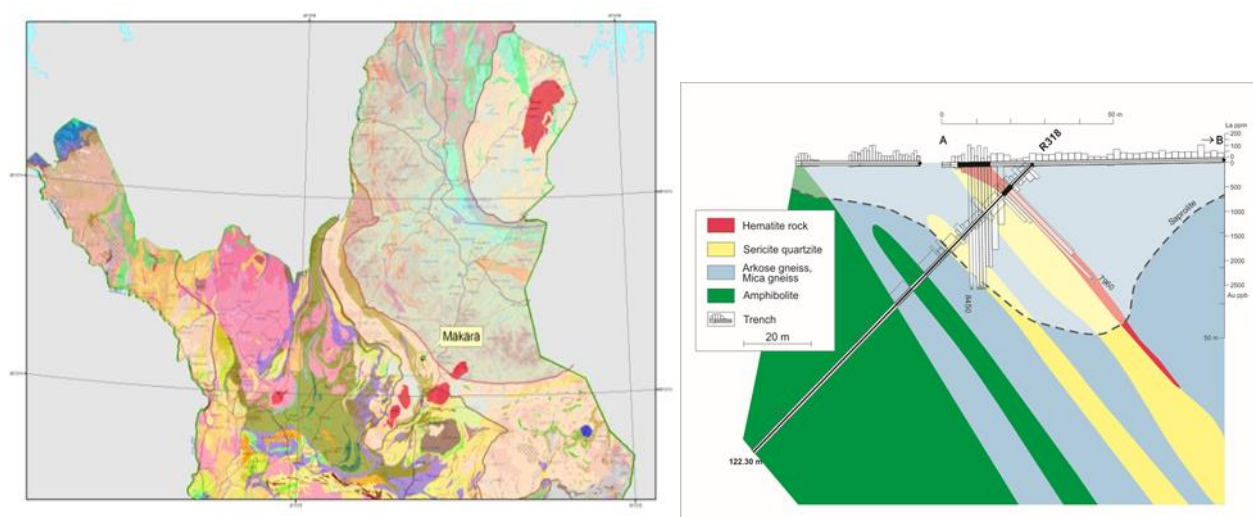

Fig 1. Location of Mäkärä Au-REE-target and a cross section of the Mäkärä drill core R318

Scope and samples

The main objectives of this study are to search gold, REE and related minerals, and to determine their associations, distributions, grain size, proportion and intergrowth with the host minerals in the rock samples taken from Mäkärä hematite-quartz-dyke and associated rocks. The other objective is to estimate the age of the Mäkärä gold deposits by using U-Pb geochronological analysis of zircon, monazite and xenotime on the thin-sections.

2   MINERALOGICAL STUDY

Four drill core samples from the drill hole R318 were submitted for mineralogical examination (Table 1). Sampling from R318 was based on chemical analyses evaluation focussing on interesting elements like Au, Th/U and related elements. According to gold assay results, the four samples indicate gold contents 1,79ppm, 1.84ppm, 7.96 ppm and 0,76ppm (Appendix I). Except with Fe, concentrations of gold have no significant correlation with other elements.

Table 1. Drill core numbers and the corresponding depth of the samples examined.

Submitted 10/03/2011	
Drill core no.	depth (m)
R318	9.50-11.00
R318	11.00-12.00
R318	12.00-13.00
R318	19.95

Hard rock sample pieces from R318 are taken at 19.95m (Fig. 1). The first three samples from drill core R318 are highly weathered (Fig. 2) and composed of pebble size pieces to dust particles, weighing 1.44kg, 1.48kg and 1.68kg, respectively. Samples are divided in to three parts for polished thin section study and comminution by selFrag and roller crusher that led to heavy minerals concentrations.
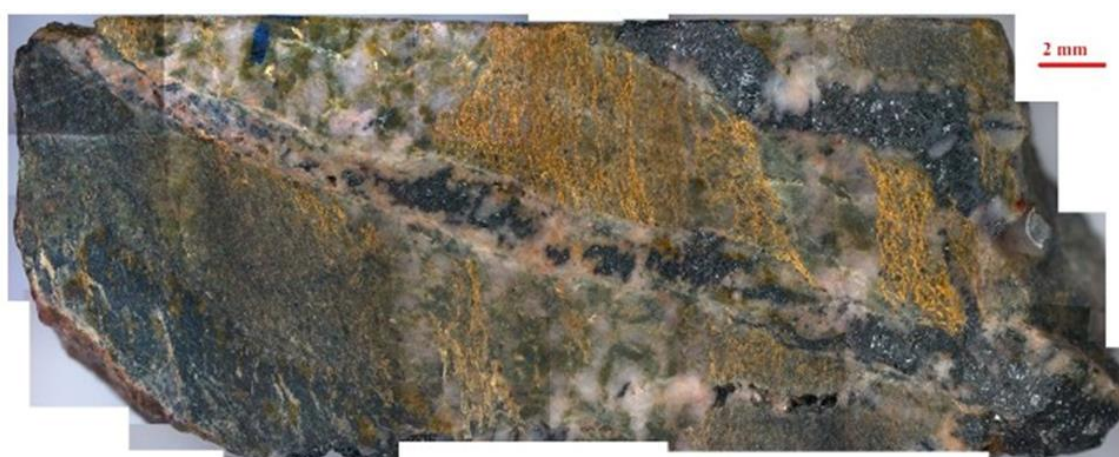

Fig 1. Hard rock sample from R318 at 19.95m. Hematite veins in sericite-quartz rock.

Fig 2. Drill core samples from R318. Samples were selected from dark grey gold-bearing hematite rich parts of cores. Yellow and reddish parts of cores are partly kaolinzed arkosic gneisses.

2.1 Sample preparation

Samples R318 (09.50-11.00), R318 (11.00-12.00) and R318 (12.00-13.00) are divided in to two portions using sample divider for comminution process with High voltage pulsed fragmentation (selFrag) and mechanical crusher (roller crusher). Two different comminution systems were used to evaluate the performance of the operation in terms of gold and other valuable minerals liberation and recovery. SelFrag was operating wet in closed system while roller crusher was operating dry with 250/300 micron sieve size. The weight of fragmented and crushed samples with produced slime is given in Table 2. Crushed sample from roller crusher was diluted with water to deslime the very fine particles. The particle size of the slime is in general <45 microns. To determine whether gold is recovered in the fine fraction (slime) or not, the fraction is sampled for chemical analyses and analysed. Fragmented (SF) and crushed (R) samples are further treated by heavy media separation (HMS) (d=3.3) to concentrate heavy minerals present. The weights of heavy and light fractions are recorded in Table 3.

Table 2. Weight of fragmented samples by selFrag (SF) and crushed samples
by roller crusher (R) and the corresponding slime

Sample ID	SF R318	SF R318 (slime)	R R318	R R318 (slime)
	(g)	(g)	(g)	(g)
9.50-11.00	309.0	166.2	359.3	154.6
11.00-12.00	393.0	120.6	428.8	87.7
12.00-13.00	318.5	151.8	368.6	135.3

Table 3. Heavy media separation (HMS), weight (g) of heavy and light fraction from
selFrag (SF) and roller crusher (R)

Sample ID	SF R318				
	weight (g)	d>3.3 (g)	d>3.3 (%)	d<3.3 (g)	hand mag (g)
9.50-11.00	309.0	75.0	24.3	228.5	5.2
11.00-12.00	393.0	264.4	67.3	128.6	2.16
12.00-13.00	318.5	109.1	34.3	208.8	0.35
Sample ID	R R318				
	weight (g)	d>3.3 (g)	d>3.3 (%)	d<3.3 (g)	hand mag (g)
9.50-11.00	359.3	70.4	19.6	288.3	0.01
11.00-12.00	428.8	255.7	59.6	172.1	0
12.00-13.00	368.6	95.0	25.8	273.1	0.05

The heavy fractions (d>3.3) are further treated by Franz electromagnetic separation and the result is presented in Table 4. Since the heavy fraction contains considerable amount of hematite and Fe hydroxides, separation was repeated with consecutive electromagnetic current (0.2A, 0.4A, 0.6A and 0.65A) to recover non-magnetic fractions that might contain gold particles. Due to the fineness of the fractions, considerable amount of fines with d<3.3 were recovered in the Franz nonmagnetic fractions. The nonmagnetic fractions were further treated by heavy liquids (methane iodide and Clerical solution) to concentrate possible gold and related minerals grains. The result of centrifuge based heavy liquid separation by clerical solution is recorded in Table 5.

Table 4. Magnetic and nonmagnetic fractions after Franz separation of heavy fractions (d>3.3)

Sample no.	SF R318					
	weight	φ > 0.33mm mag	Franz (mag)			d> 3.3 Nmag
	(g)		0.2A	0.6A	0.4A	
9.50-11.00	75.0	5.9	39.2	17.5	-	12.4
11.00-12.00	264.4	-	191.7	-	40.8	31.9
12.00-13.00	109.1	6.2	61.5	16.4	-	25.0
Sample no.	R R318					
	weight	φ > 0.33mm mag	Franz (mag)			d> 3.3 Nmag
	(g)		0.2A	0.6A	0.5A	
9.50-11.00	70.4	1.85	24.5	36.4	-	7.7
11.00-12.00	255.7	-	221.8	-	-	33.9
12.00-13.00	95.0	1.1	27.3	-	55.7	10.9

Note: The nonmagnetic (Nmag) fractions still contain a lot of fines with d<3.3

Table 5. Centrifuge heavy media separation using clerical solution

Sample no.	SF R318 d>3.3, Franz Nmag, centrifuge separation		
	d> 3.3 Nmag	d=3.3-4.0 (g)	Clerical d> 4.0 (g)
9.50-11.00	12.4	1.0	0.14
11.00-12.00	31.9	0.1	0.04
12.00-13.00	25.0	1.1	0.04
Sample no.	R R318 d>3.3, Franz Nmag, centrifuge separation		
	d> 3.3 Nmag	d>3.3 (g)	Clerical d> 4.0 (g)
9.50-11.00	7.65	0.7	-
11.00-12.00	33.9	1.2	1.15
12.00-13.00	10.9	0.9	0.16

The nonmagnetic heavy mineral concentrates (d>4.0) are studied under SEM (Jeol 5900LV). In this case, powder samples are carefully prepared on a carbon tap for gold and related minerals search. SEM was aided by software called 'INCA FEATURE' that was able to search gold grains and related minerals down to 2 to 3microns. Several images were taken along with semi-quantitative analyses of the detected heavies with the EDS unit.

Polished thin sections (R318-19.95m) are studied both in transmitted and reflected light microscope (Leitz DMRP) equipped with digital camera (Leica DFC 490 + Leica Application Software). Microphotographs of the ore and rock forming minerals were taken to illustrate mineral distribution and texture. Gold and associated minerals, however, are very fine grained, beyond petrographic microscope observation. Hence, polished sections are examined under the scanning electron microscope (SEM) attached with software FEATURE for gold and related minerals search. Scanning with electron microscope also supported to observe textural configuration of the rare minerals in the rock. Several BSE images were taken along with semi-quantitative analyses of the ore minerals with the EDS detecting unit.

Large grains of monazite and xenotime were delineated and analyzed for dating (U/Pb) using LAICPMS directly from polished thin sections. EMPA (using Cameca SX100) was also conducted on the same dated Monazite and xenotime grains. The analytical conditions for monazite and xenotime analyses were 15 kV acc. voltage, 10 nA beam current and 5 micrometers beam diameter.

2.2 Sample analyses

Light microscope observation

The major rock forming mineral assemblage is dominated by muscovite-sericite-chlorite associated with quartz and altered feldspar (Fig 3). Opaque minerals are composed of hematite (goethite/ limonite), Fe-Ti minerals, with minor sulphides and magnetite. Under cross polarized light, hematite display two distinct occurrence, acicular crystals with abundant twinning and intergrown with rutile (Figs 4).
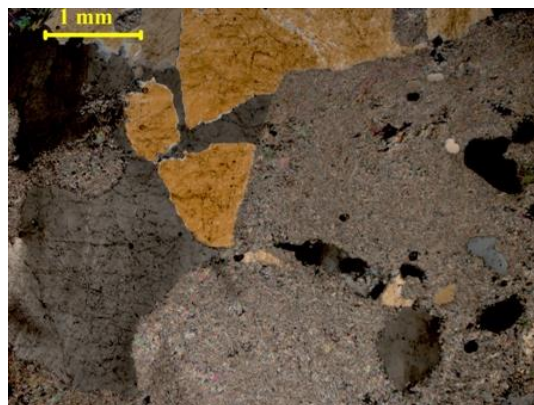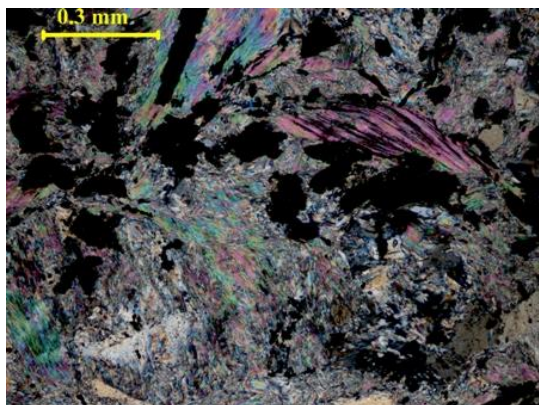
Fig 3. Rock forming minerals mainly of sericite-muscovite-chlorite-qtz and altered feldspar (alteration assemblage) (R318-19.95)
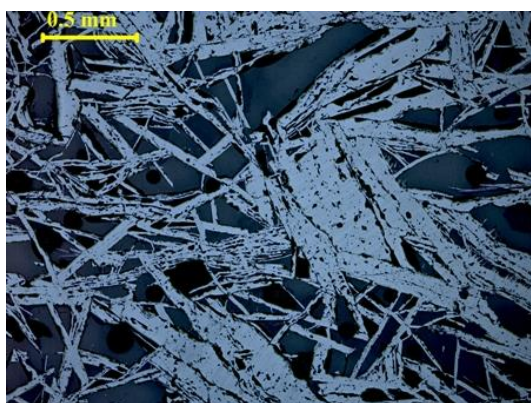
Fig 4. a) Acicular/lenticular hematite with twinning structure, and b) hematite-rutile intergrowth (R318-19.95)

Scanning electron microscope observation

Polished thin section (R318-19.95m)

During gold search, electron microscope study revealed a number of important heavy minerals including REE bearing that were beyond the limit of observation under binocular light microscope. Apart from acicular hematite (Fig. 5a) and hematite-rutile intergrowths (Fig. 5b), disseminated to aggregated grains of zircon, monazite and xenotime are observed (Fig. 6 and 7). Other rarely occurring heavy minerals are fine grained gold (3-5 microns) (Fig.6a), sulphide minerals mainly chalcopyrite and Cu and Zn bearing silicates (Fig 5a, b).

Fig. 5 a) Acicular hematite associated with quartz grains, b) Hematite- rutile intergrowth
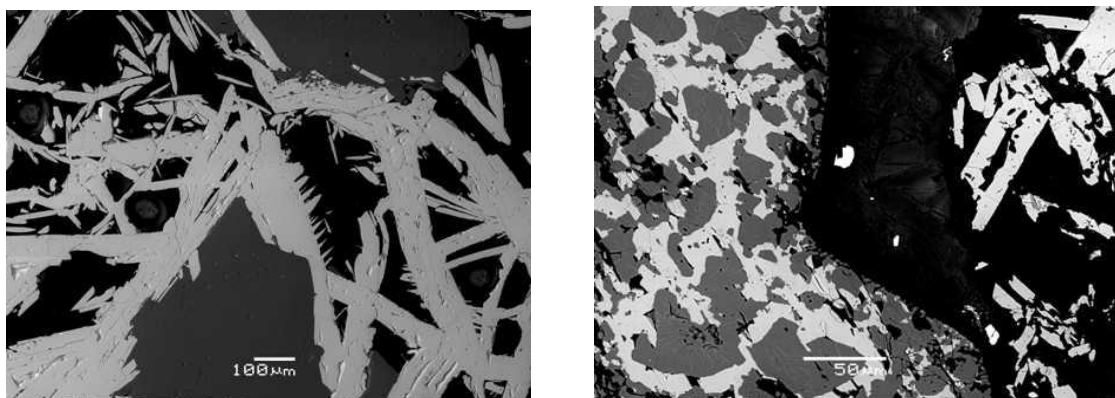
Monazite grains are often associated and intergrown with rutile and grain size varied from a few microns up to 100 microns. Semi quantitative analyses with SEM EDS shows that monazite is containing 19.5-29.3 wt. % Ce, 5.1-11.4 wt. % of La, 11.4-16.5 wt. % of P, 8.1-12.4 wt. % Nd and considerable amount of Fe. According to the given composition monazite is largely of Ce variety (Ce-monazite) with trace amount of Th and Sm.

A few grains of xenotime are encountered in polished thin sections, mainly associated with hematite. The grains shape varied from anhedral/ irregular to euhedral with crystal structures and zonings (Fig. 8). The grain size varied from a few microns to about 100 microns. The composition of xenotime according to SEM-EDS analyses is Y-xenotime with Y_2O_3 varied from 34.6-43.5 wt. % and P_2O_3 varies from 33.6 to 38.6 wt. %. Xenotime with relatively lower content of Y and P contains trace amount of Eu and Gd.
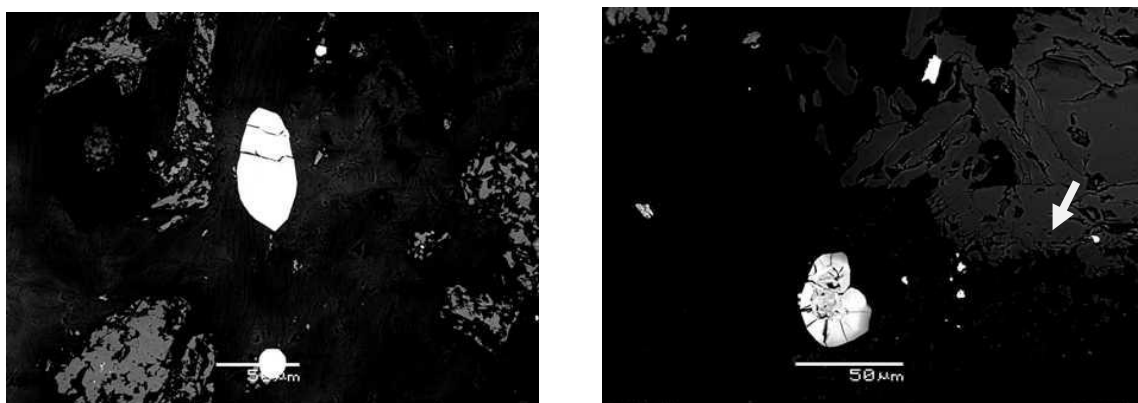

Fig. 6. a) Zircon grains (light), rutile aggregates (dark grey) within muscovite sericite alteration assemblage, b) zircon, monazite grains (light), hematite (dark grey)) and gold particle within hematite mass (see arrow)
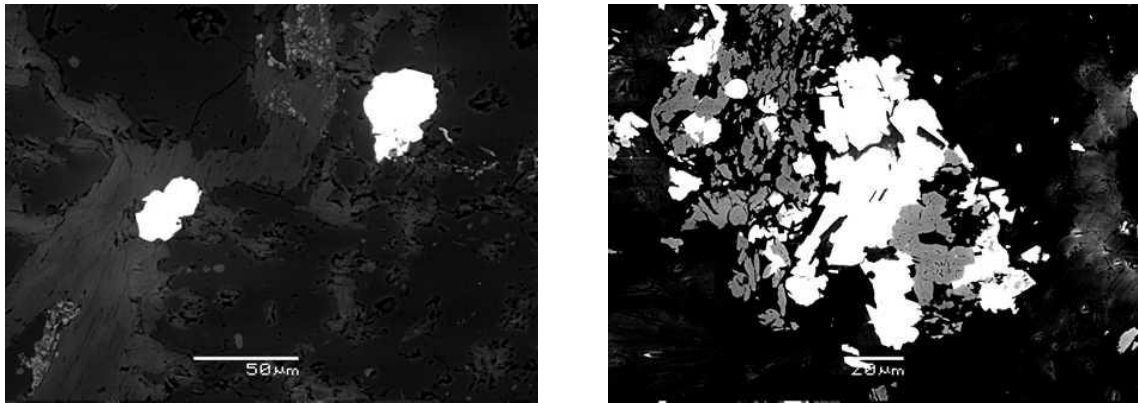
Fig. 7a) Monazite (light), rutile (light grey), muscovite-sericite (dark grey), quartz (dark), b) Monazite aggregates associated with rutile grains, and a few grains of zircons with the muscovite-sericite-quartz ground mass.

Fig. 8a) Large grains of xenotime (light) zircon grain (light grey) and hematite mass (dark grey), b) Zoned xenotime crystal within acicular hematite aggregates

Heavy mineral concentrates (R318- 11.00-12.00)

Heavy minerals are concentrated from R318 (9.5-11.00), R318 (11.00-12.00) and R318 (12.00-13.00). However, the result presented here is from R318 (11.00-12.00), the only sample from which free gold grains are encountered. In spite of the influence by the comminution methods used, crushed/fragmented hematite displays various types of shapes from flaky to granular and angular to subrounded (Figs. 9-14). A few grains of gold are found in the heavy mineral concentrates (R318 (11.00-12.00)) ranging in size from 40 to 70 microns (Fig. 9-14). The gold particles display spongy or coral reef like structure to skeletal or dendritic structures. The composition, according to SEM-EDS, indicates rather pure gold with trace amount of Ag and Fe. Most of the Fe composition might have derived from the spectrum of the surrounding hematite grains.
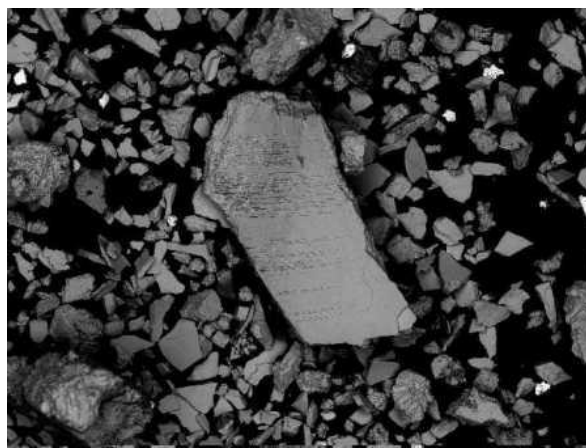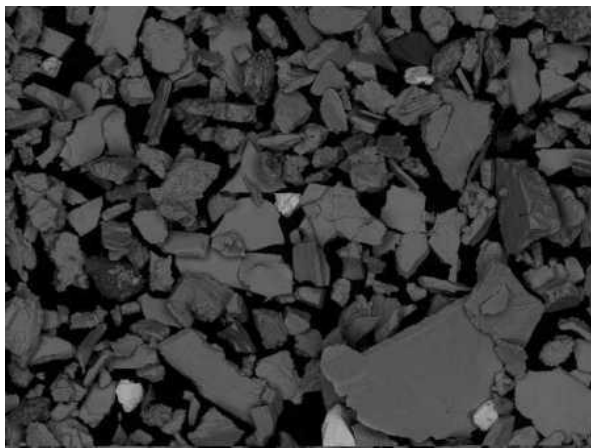
Fig. 9. Heavy mineral concentrate dominated by hematite with minor amount of rutile and monazite. Note the flaky shape of hematite (a) 0.7 mm across (b) 1.2 mm across (Roller, R318 11.00-12.00)
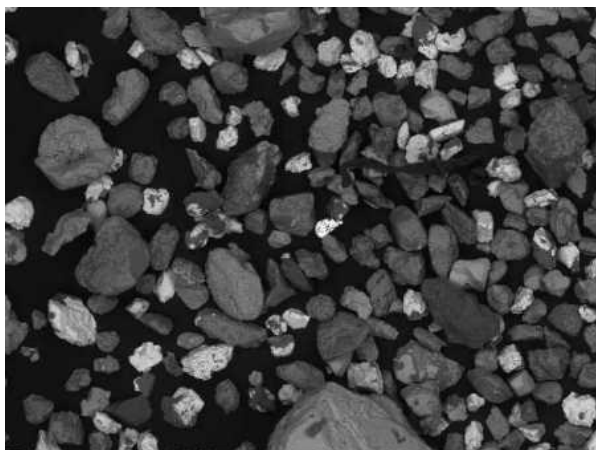
Fig.10. Heavy mineral concentrate dominated by hematite and monazite with some rutile, zircon, xenotime and silicates (1 mm across) (SF R318-11.00-12.00)
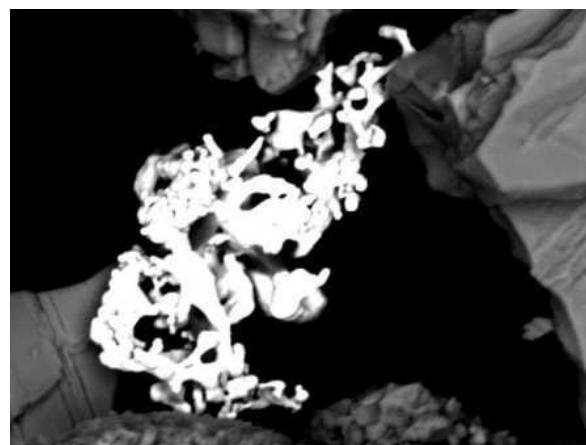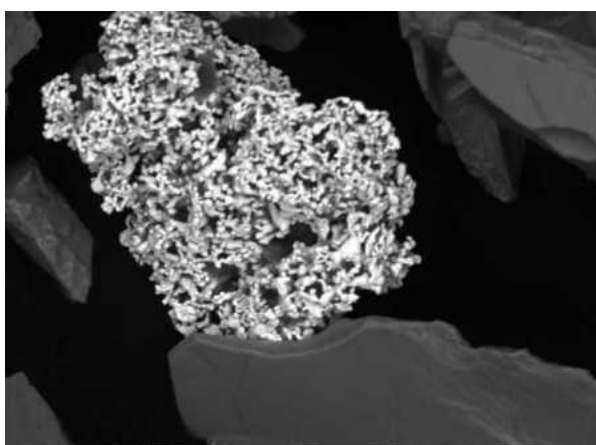
Fig. 11. Gold grain with reef like structure (50µm), b) Skeletal/dendrtic type of gold (40µm) composition Au= 81-89 wt. %, Fe= 10-18 wt. % (Roller, R318 11.00-12.00)
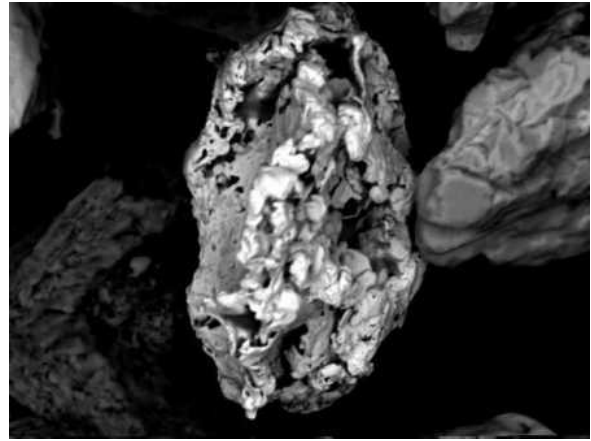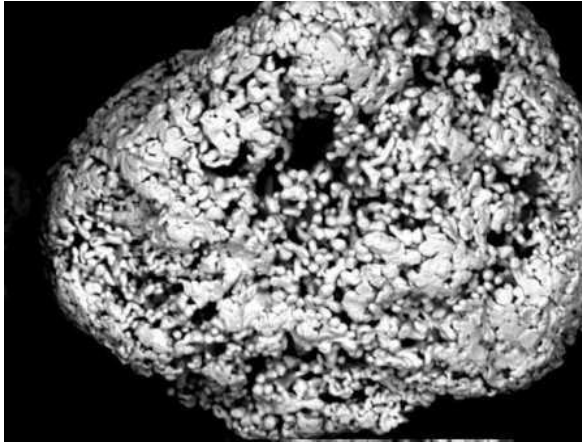
Fig. 12 a) Gold reef like structure (70 μm) b) Compositionally varying Au up to 97 wt. % with trace Fe & Ag, bright – contains no Ag, grey - Au with 4-5wt. % of Ag. (SF R318 11.00-12.00)
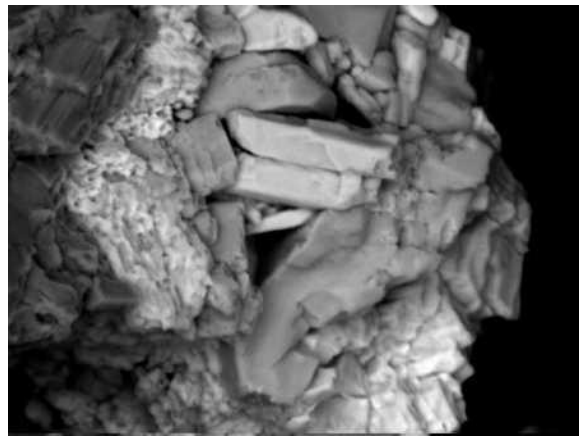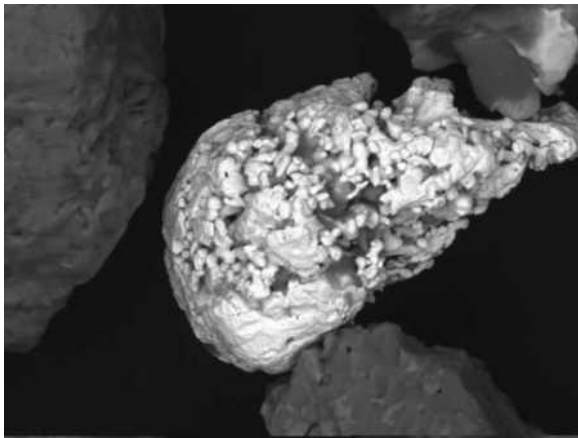
Fig.13 a) Gold grain with high purity (50μm) (Au= 96-97 wt. %, Fe=3-3.5 wt. %), b) Aggregates of monazite, xenotime, zircon and hematite (from core to outer surface) (60μm across) (SF R318 11.00-12.00)
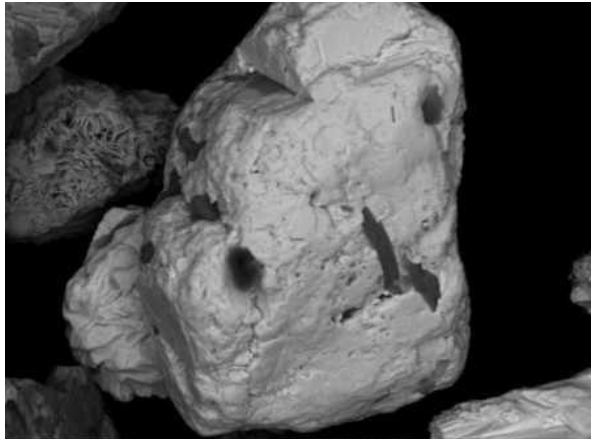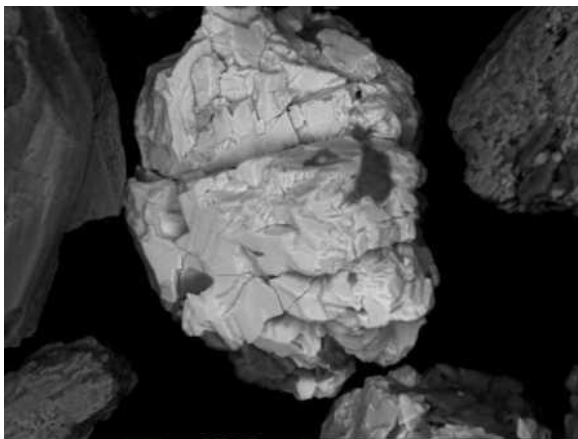
Fig. 14. Monazite grains (90 - 100μm in size) ((SF R318 11.00-12.00)

Monazite is the most common heavy mineral next to hematite (Figs. 13-14). The liberated particle size ranges from a few microns to about 100 microns. Intergrowth of monazite with xenotime and hematite is rarely observed (Fig. 14). Monazite is often associated with rutile and liberated particles of monazite still containing fine grained rutile crystals.

Chemical analyses of the slime for Gold

The weight of selFrag fragmented and roller crusher crushed samples with produced slime is given in Table 2. Crushed sample from roller crusher that was operated dry was diluted with water to deslime the very fine particles. To determine whether gold is recovered in the fine fraction (slime) or not, the fraction is sampled for chemical analyses and analysed (Table 6). The particle size of deslimed material is in general <45 microns, from both grinding application.

Table 6. Chemical analyses of slime, for gold, produced from selFrag and roller crusher (ICP-AES)

Customer Sample ID	Au µg/kg +704P	Au ppm	fragmenting/ crushing menthod
R318 (9.50-11.00)	6480	6,48	selFrag
R318 (9.50-11.00)	4010	4,01	roller crusher
R318 (11.00-12.00)	20200	20,2	selFrag
R318 (11.00-12.00)	12500	12,5	roller crusher
R318 (12.00-13.00)	1870	1,87	selFrag
R318 (12.00-13.00)	2320	2,32	roller crusher

The deslimed material from both applications contains considerable amount of gold particles. This might be indicating either gold is primarily very fine grained in the ore or comminution might have an effect. It is also possible that high Au content in the slime from selFrag might indicate better liberation of fine particles considering no particle breakage. However, the content of the gold in each slime samples is proportional to the Au content of the corresponding drill core sample (uncrushed material, Appendix I).

2.3 Electron microprobe analyses (EMPA)

Electron microprobe analysis was conducted on zircon, monazite and xenotime particles that were delineated by SEM for LA-ICPMS analysis, U/Pb age determination.

Table 7. EMPA of zircon, monazite and xenotime from R318-19.95m (wt. %)

Zircon (Weight-%)

SiO2	TiO2	Al2O3	V2O3	FeO	MgO	CaO	K2O	Cs2O	SnO2	PbO	UO2	ThO2	SO2	WO3	Sc2O3	HfO2	Y2O3	ZrO2	Ce2O3	Pr2O3	F	Cl	Total
34.24	0.09	0.00	0.01	0.14	0.00	0.01	0.04	0.00	0.00	0.00	0.00	0.00	0.04	0.09	0.01	1.17	0.00	**61.38**	0.11	0.00	0.10	0.00	97.43
36.09	0.05	0.03	0.00	0.09	0.00	0.00	0.05	0.00	0.02	0.00	0.00	0.00	0.07	0.00	0.02	1.24	0.00	**59.46**	0.04	0.14	0.01	0.04	97.34
32.78	0.08	0.61	0.00	0.40	0.01	0.10	0.18	0.04	0.05	0.00	0.00	0.08	0.06	0.00	0.03	1.38	0.53	**60.41**	0.13	0.29	0.02	0.00	97.17
28.37	0.10	0.41	0.09	0.53	0.04	0.19	0.02	0.01	0.00	0.04	0.03	0.21	0.04	0.38	0.17	1.20	3.07	**59.30**	0.25	0.09	0.13	0.01	94.69

Monazite (Weight %)

SiO2	TiO2	Al2O3	FeO	MnO	MgO	CaO	K2O	Cs2O	PbO	UO2	ThO2	P2O5	Nb2O5	WO3	HfO2	Y2O3	Ce2O3	Nd2O3	La2O3	Pr2O3	F	Cl	Total
0.18	0.11	0.00	0.00	0.00	0.00	0.09	0.03	**0.46**	0.00	0.00	0.05	**29.14**	0.08	0.00	0.05	0.35	**32.77**	**14.94**	**13.35**	**5.70**	0.58	0.06	97.93
0.19	0.00	0.05	0.02	0.02	0.00	0.13	0.02	**0.39**	0.00	0.18	0.00	**29.13**	0.03	0.20	0.19	0.52	**32.33**	**15.61**	**13.42**	**5.68**	0.73	0.06	98.95
0.19	0.04	0.00	0.00	0.09	0.02	0.13	0.00	**0.45**	0.10	0.02	0.04	**28.95**	0.06	0.09	0.00	0.41	**32.18**	**15.20**	**13.39**	4.93	0.71	0.03	97.03
0.27	0.10	0.00	0.00	0.05	0.00	0.12	0.00	**0.45**	0.00	0.00	0.02	**28.77**	0.00	0.00	0.00	0.31	**31.90**	**17.70**	**11.28**	**5.97**	0.53	0.08	97.54
0.27	0.00	0.00	0.00	0.13	0.03	0.20	0.00	**0.38**	0.10	0.00	0.14	**28.47**	0.02	0.07	0.00	0.13	**32.13**	**17.20**	**12.04**	**5.45**	0.66	0.06	97.47
0.20	0.02	0.02	0.00	0.01	0.02	0.17	0.00	0.45	0.16	0.00	0.97	**29.10**	0.11	0.00	0.00	0.33	**32.12**	14.55	13.23	**5.39**	0.68	0.06	97.60
0.22	0.00	0.03	0.00	0.00	0.00	0.33	0.05	0.37	0.00	0.19	0.02	**28.61**	0.00	0.00	0.13	0.32	**33.26**	16.77	10.95	**6.41**	0.68	0.04	98.38
0.24	0.08	0.00	0.00	0.00	0.00	0.63	0.00	0.48	0.10	0.08	0.13	**28.35**	0.00	0.34	0.16	0.21	**33.41**	**15.61**	**12.46**	5.49	0.70	0.04	98.51
0.40	0.01	0.14	0.00	0.00	0.00	0.09	0.03	0.44	0.09	0.21	0.30	**28.39**	0.00	0.15	0.00	0.11	**33.43**	13.24	**14.85**	5.33	0.66	0.06	97.93
0.27	0.12	0.05	0.00	0.08	0.00	0.13	0.35	0.44	0.00	0.13	0.09	**28.70**	0.00	0.00	0.00	0.37	**30.95**	**15.28**	**11.72**	5.98	0.62	0.10	95.37
0.33	0.06	0.06	0.00	0.05	0.05	0.13	0.44	0.39	0.24	0.33	0.07	**29.11**	0.10	0.22	0.00	0.28	**30.34**	**15.03**	**11.26**	5.66	0.46	0.16	94.76
0.23	0.97	0.00	0.00	0.08	0.00	0.58	0.07	0.44	0.01	0.00	0.39	**29.58**	0.00	0.07	0.27	0.31	**31.97**	14.74	**12.33**	5.71	0.61	0.05	98.40
3.81	2.53	2.63	0.19	0.05	0.14	0.29	0.83	0.40	0.00	0.11	0.13	**26.92**	0.09	0.00	0.21	0.31	**30.02**	**12.31**	**12.18**	4.42	0.53	0.03	98.12
0.34	0.97	0.00	0.02	0.08	0.08	0.58	0.11	0.42	0.00	0.18	0.43	**29.16**	0.06	0.24	0.00	0.39	**30.59**	**13.71**	**12.21**	5.20	0.61	0.08	95.44
0.29	0.63	0.01	0.16	0.00	0.02	0.52	0.08	0.38	0.09	0.09	0.55	**29.26**	0.00	0.00	0.06	0.23	**30.69**	**13.55**	**12.29**	5.63	0.56	0.10	95.18
0.66	2.66	0.09	0.04	0.04	0.00	0.43	0.17	0.45	0.00	0.00	0.56	**29.81**	0.00	0.17	0.00	0.34	**30.80**	**12.70**	**12.35**	4.67	0.49	0.02	96.44

Note: BaO = 0.0-0.1, SnO2=0.0-0.04, SO2=0.0-0.13

Xenotime (Weight %)

SiO2	TiO2	V2O3	FeO	MnO	CaO	K2O	SrO	BaO	Cs2O	PbO	UO2	ThO2	SO2	P2O5	Nb2O5	WO3	HfO2	Y2O3	Ce2O3	Nd2O3	F	Cl	Total
0.19	0.01	0.00	0.00	0.00	0.02	0.00	0.01	0.06	0.02	0.30	0.04	0.10	0.04	**31.66**	0.11	**3.31**	0.39	**33.79**	0.16	0.12	0.10	0.01	**70.44**
0.21	0.08	0.00	0.00	0.07	0.05	0.00	0.06	0.08	0.00	0.16	0.24	0.15	0.00	**30.36**	0.07	**3.65**	0.28	**33.66**	0.11	0.07	0.07	0.01	**69.36**
0.38	0.00	0.04	0.00	0.00	0.04	0.00	0.02	0.00	0.00	0.46	0.00	0.05	0.02	**31.29**	0.09	2.86	0.51	33.70	0.12	0.04	0.10	0.00	**69.72**
0.62	0.00	0.02	0.00	0.00	0.07	0.18	0.06	0.16	0.02	0.48	0.00	0.13	0.05	**33.31**	0.05	1.96	0.41	36.27	0.00	0.15	0.00	0.05	**73.99**
0.68	0.00	0.00	0.00	0.01	0.04	0.13	0.00	0.00	0.00	0.22	0.00	0.12	0.00	**33.22**	0.00	2.02	0.38	36.03	0.03	0.13	0.02	0.01	**73.03**
0.14	0.00	0.03	0.00	0.07	0.03	0.01	0.08	0.18	0.00	0.24	0.00	0.05	0.00	**31.92**	0.00	**2.45**	0.41	**37.14**	0.08	0.03	0.02	0.01	**72.89**
0.14	0.00	0.00	0.00	0.05	0.08	0.00	0.08	0.05	0.00	0.40	0.00	0.16	0.01	**31.51**	0.00	2.94	0.61	**33.17**	0.03	0.07	0.03	0.00	**69.36**
0.05	0.02	0.01	0.00	0.00	0.07	0.03	0.00	0.00	0.00	0.37	0.05	0.00	0.08	**32.88**	0.09	2.64	0.38	**37.80**	0.05	0.03	0.10	0.01	**74.64**
0.00	0.00	0.12	0.00	0.03	0.02	0.00	0.00	0.00	0.04	0.21	0.00	0.08	0.03	**31.95**	0.07	2.53	0.45	**35.17**	0.19	0.09	0.01	0.00	**70.99**
0.10	0.00	0.10	0.00	0.04	0.00	0.00	0.00	0.11	0.02	0.45	0.19	0.28	0.00	**31.21**	0.19	2.79	0.21	**33.21**	0.16	0.00	0.00	0.00	**69.07**
0.10	0.00	0.00	0.00	0.08	0.03	0.00	0.06	0.11	0.00	0.27	0.01	0.02	0.01	**31.13**	0.08	2.90	0.52	**33.77**	0.10	0.00	0.03	0.00	**69.22**
0.25	0.00	0.00	0.46	0.00	0.00	0.00	0.08	0.04	0.10	0.09	0.23	0.55	0.03	**30.26**	0.00	3.28	0.25	**33.48**	0.06	0.22	0.03	0.00	**69.40**
0.14	0.00	0.00	0.00	0.01	0.01	0.00	0.01	0.03	0.03	0.35	0.28	0.52	0.03	**30.47**	0.00	2.95	0.40	34.32	0.12	0.00	0.14	0.02	**69.84**
0.11	0.07	0.00	0.00	0.04	0.02	0.00	0.02	0.14	0.01	0.12	0.00	0.08	0.03	**31.46**	0.14	2.58	0.97	**35.41**	0.07	0.00	0.00	0.00	**71.27**
0.16	0.00	0.01	0.00	0.00	0.02	0.00	0.00	0.00	0.01	0.14	0.08	0.26	0.00	**31.05**	0.04	3.02	0.60	35.28	0.00	0.07	0.00	0.00	**70.74**

Note: NaO2=0.0-0.09, SnO2=0.0-0.06, Sc2O3=0.0-0.06

Monazite is a Ce- variety. Apart from Neodymium (Nd) it contains considerable amount of Praseodymium (Pr), and trace amount of Cs_2O, Y_2O_3, ThO_2, F and Cl. Quantitative analyses of the given xenotime grains here are failed as the sum is quite low. This is believed to be the grains were being damaged by LAICPMS for dating. There was no enough space of the electron beam outside the

crater caused by laser drilling. Hence, EMP analyses should be performed before on such grains before dating. Nevertheless, xenotime seems to contain considerable amount of WO_3 and HfO_2, and trace amount of PbO, CeO_3, Nd_2O_3, ThO_2 and UO_2.

3 U-PB GEOCHRONOLOGICAL ANALYSIS OF ZIRCON, MONAZITE AND XENOTIME

3.1 Analytical technique

U-Pb dating analyses were performed using a Nu Plasma HR multicollector ICPMS at the Geological Survey of Finland in Espoo using a technique very similar to Rosa et al (2009) except that a Photon Machine Analyte G2 laser microprobe was used. Samples were ablated in He gas (gas flows = 0.4 and 0.1 l/min) within a HelEx ablation cell (Müller et al., 2009). He aerosol was mixed with Ar (gas flow= 1.0 l/min) prior to entry into the plasma. The gas mixture was optimized daily for maximum sensitivity. All analyses were made in static ablation mode on thin sections. Ablation normal conditions were: beam diameter: 6μm; pulse frequency: 5 Hz; beam energy density: 0.55 J/cm^2. A single U-Pb measurement included 20 s of on-mass background measurement, followed by 30-60s of ablation with a stationary beam. Masses 204, 206 and 207 were measured in secondary electron multipliers, and 238 in the extra high mass Faraday collector. The geometry of the collector block does not allow simultaneous measurement of 208Pb and 232Th. Ion counts were converted and reported as volts by the Nu Plasma time-resolved analysis software. 235U was calculated from the signal at mass 238 using a natural 238U/235U=137.88. Mass number 204 was used as a monitor for common 204Pb. In an ICPMS analysis, 204Hg originates mainly from the He supply. The observed background counting-rate on mass 204 was ca. 1200 (ca. 1.3×10-5 V), and has been stable at that level over the last year. The contribution of 204Hg from the plasma was eliminated by on-mass background measurement prior to each analysis. Age related common lead (Stacey and Kramers, 1975) correction was used when the analysis showed common lead contents above the detection limit. Signal strengths on mass 206 were typically > 10-3 V, depending on the uranium content and age of the zircon. Two calibration monazite standards and one monazite standard were run in duplicate at the beginning and end of each analytical session, and at regular intervals during sessions.

Zircon: Raw data were corrected for the background, laser induced elemental fractionation, mass

discrimination and drift in ion counter gains and reduced to U-Pb isotope ratios by calibration to concordant reference zircons of known age, using protocols adapted from Andersen et al. (2004) and Jackson et al. (2004). Standard zircons GJ-01 (609 ± 1 Ma; Belousova et al. 2006) and an in-house standard A1772 (2712±1 Ma, Huhma et al, 2012) were used for calibration.

Monazite: Raw data were corrected for background, laser induced elemental fractionation, mass discrimination and drift in ion counter gains and reduced to U-Pb isotope ratios by calibration to concordant reference monazite of known age, using protocols adapted from Andersen et al. (2004) and Jackson et al. (2004). In-house monazite standards A49 (1874 ± 3 Ma) and A1326 (2635 ± 2 Ma; Hölttä et al 2000) were used for calibration. The in-house monazite sample A276 has also been used for quality control (Meriläinen K. 1976, 1911 ± 5 Ma, TIMS unpublished data).

Xenotime: A single in house xenotime standard A1298 (1852 Ma, TIMS age, Pajunen and Poutiainen (1999) was used for calibration.

The calculations were done off-line, using an interactive spreadsheet program written in Microsoft Excel/ VBA by T. Andersen (Rosa et al, 2009). To minimize the effects of laser-induced elemental fractionation, the depth-to-diameter ratio of the ablation pit was kept low, and isotopically homogeneous segments of the time-resolved traces were calibrated against the corresponding time interval for each mass in the reference standard. To compensate for drift in instrument sensitivity and Faraday vs. electron multiplier gain during an analytical session, a correlation of signal vs. time was assumed for the reference zircons. A description of the algorithms used is provided in Rosa et al (2009). Plotting of the U-Pb isotopic data and age calculations were performed using the Isoplot/Ex 4.15 program (Ludwig, 2003). All the ages were calculated with 2σ errors and without decay constants errors. Data-point error ellipses in the figures are at the 2σ level. The concordant age offset from ID-TIMS ages for several samples does not exceed 0.5%.

3.2 Laser Ablation ICP MS dating on Mäkärä's dyke

The analytical results are presented in Table 8. The figures in the next pages conclude the xenotime, monazite and zircon dating results for the Mäkärä's gold-bearing vein (Figs 15-17).

Table 8. LA-MC-ICPMS U-Pb analyses

| Name	ppm U	^{206}Pb	^{206}Pb$_c$(%)	^{206}Pb/^{204}Pb	^{207}Pb/^{206}Pb*	1σ	^{207}Pb/^{235}U*	1σ	^{206}Pb/^{238}U*	1σ	Rho	Discordance Central (%)	^{207}Pb/^{206}Pb	1σ	^{207}Pb/^{235}U	1σ	^{206}Pb/^{238}U	1σ
Zircon																		
RO1151-zirc10	48	29	0.00	12557	0.16418	0.00084	10.246	0.417	0.4526	0.0183	0.99	-4.4	2499	8	2457	38	2407	81
RO1155-zirc4	105	54	0.18	22960	0.13727	0.00079	7.739	0.303	0.4089	0.0159	0.99	0.9	2193	10	2201	35	2210	73
RO1155-zirc5	115	57	0.02	11550	0.14126	0.00114	7.754	0.279	0.3981	0.0140	0.97	-4.3	2243	13	2203	32	2160	64
R318-19.95a					0.11575	0.00090	5.082	0.258	0.3185	0.0160	0.99	-6.6	1892	14	1833	43	1782	78
R318-19.95a					0.11656	0.00123	4.453	0.243	0.2771	0.0149	0.98	-19.4	1904	18	1722	45	1577	75
Monazite																		
R318-19.95b					0.10906	0.00166	5.250	0.342	0.3491	0.0221	0.97	9.5	1784	27	1861	55	1930	106
R318-19.95b					0.10990	0.00170	5.110	0.288	0.3372	0.0182	0.96	4.8	1798	28	1838	48	1873	88
R318-19.95b					0.11014	0.00173	5.111	0.291	0.3366	0.0184	0.96	4.4	1802	28	1838	48	1870	89
R318-19.95b					0.11041	0.00174	5.105	0.309	0.3353	0.0196	0.97	3.7	1806	28	1837	51	1864	95
R318-19.95b					0.11135	0.00177	5.028	0.298	0.3275	0.0187	0.96	0.3	1822	28	1824	50	1826	91
R318-19.95b					0.11109	0.00179	5.086	0.301	0.3320	0.0189	0.96	1.9	1817	29	1834	50	1848	91
R318-19.95b					0.11260	0.00184	5.143	0.310	0.3313	0.0192	0.96	0.2	1842	29	1843	51	1845	93
Xenotime																		
RO1153-xeno-2a	84	0.9	0.00	3924	0.11178	0.00069	5.250	0.168	0.3406	0.0107	0.98	3.9	1829	11	1861	27	1890	51
RO1153-xeno-2c	157	1.8	0.00	9907	0.11203	0.00087	5.207	0.157	0.3371	0.0098	0.97	2.5	1833	14	1854	26	1873	47
RO1153-xeno-2b	154	1.8	0.02	5199	0.11561	0.00069	5.431	0.137	0.3407	0.0083	0.97	.	1889	11	1890	22	1890	40
R3-1076-xeno-4b	89	0.9	0.08	4162	0.10801	0.00094	4.862	0.188	0.3265	0.0123	0.98	3.6	1766	15	1796	33	1821	60
R3-1076-xeno-4a	92	0.9	0.00	5443	0.10823	0.00095	4.769	0.185	0.3196	0.0121	0.97	1.2	1770	15	1780	33	1788	59
RO1153-xeno-4b	546	5.6	0.00	110476	0.10859	0.00059	4.661	0.114	0.3113	0.0074	0.98	-1.9	1776	9	1760	20	1747	36
RO1153-xeno-4a	154	1.6	0.00	6718	0.10977	0.00068	4.766	0.111	0.3149	0.0071	0.96	-2.0	1796	11	1779	20	1765	35
R318-19.95b					0.10591	0.00052	3.955	0.069	0.2708	0.0045	0.96	-12.0	1730	9	1625	14	1545	23
R318-19.95b					0.10699	0.00055	4.137	0.073	0.2804	0.0047	0.96	-10.0	1749	9	1662	14	1593	24
R318-19.95b					0.10651	0.00055	4.139	0.073	0.2819	0.0048	0.96	-9.1	1741	9	1662	14	1601	24
R318-19.95b					0.10657	0.00057	4.143	0.082	0.2819	0.0054	0.96	-9.1	1742	9	1663	16	1601	27
R318-19.95b					0.10637	0.00057	4.311	0.079	0.2939	0.0051	0.96	-5.0	1738	9	1695	15	1661	26
R318-19.95b					0.10759	0.00060	4.216	0.084	0.2842	0.0054	0.96	-9.4	1759	10	1677	16	1613	27
R318-19.95b					0.10764	0.00059	4.088	0.071	0.2754	0.0046	0.95	-12.3	1760	10	1652	14	1568	23
R318-19.95b					0.10702	0.00060	4.084	0.072	0.2768	0.0046	0.95	-11.2	1749	10	1651	14	1575	23
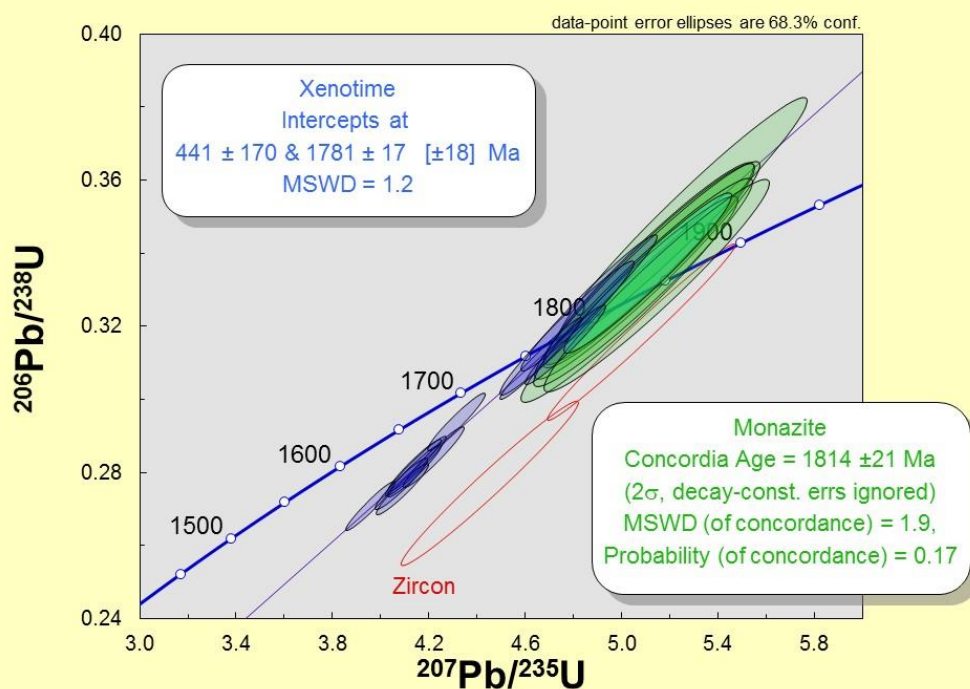
Fig 15.
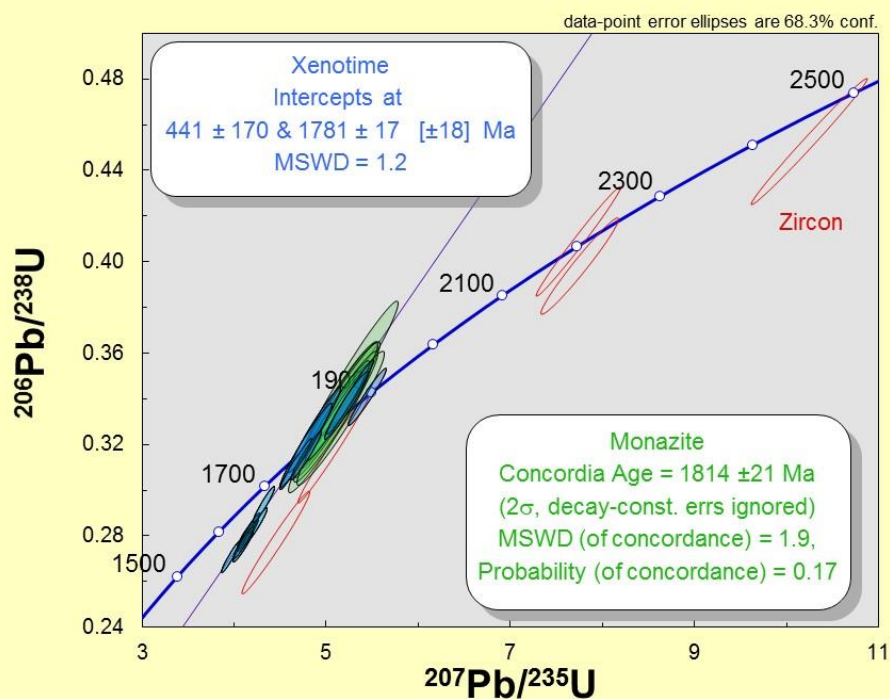
Fig 16.
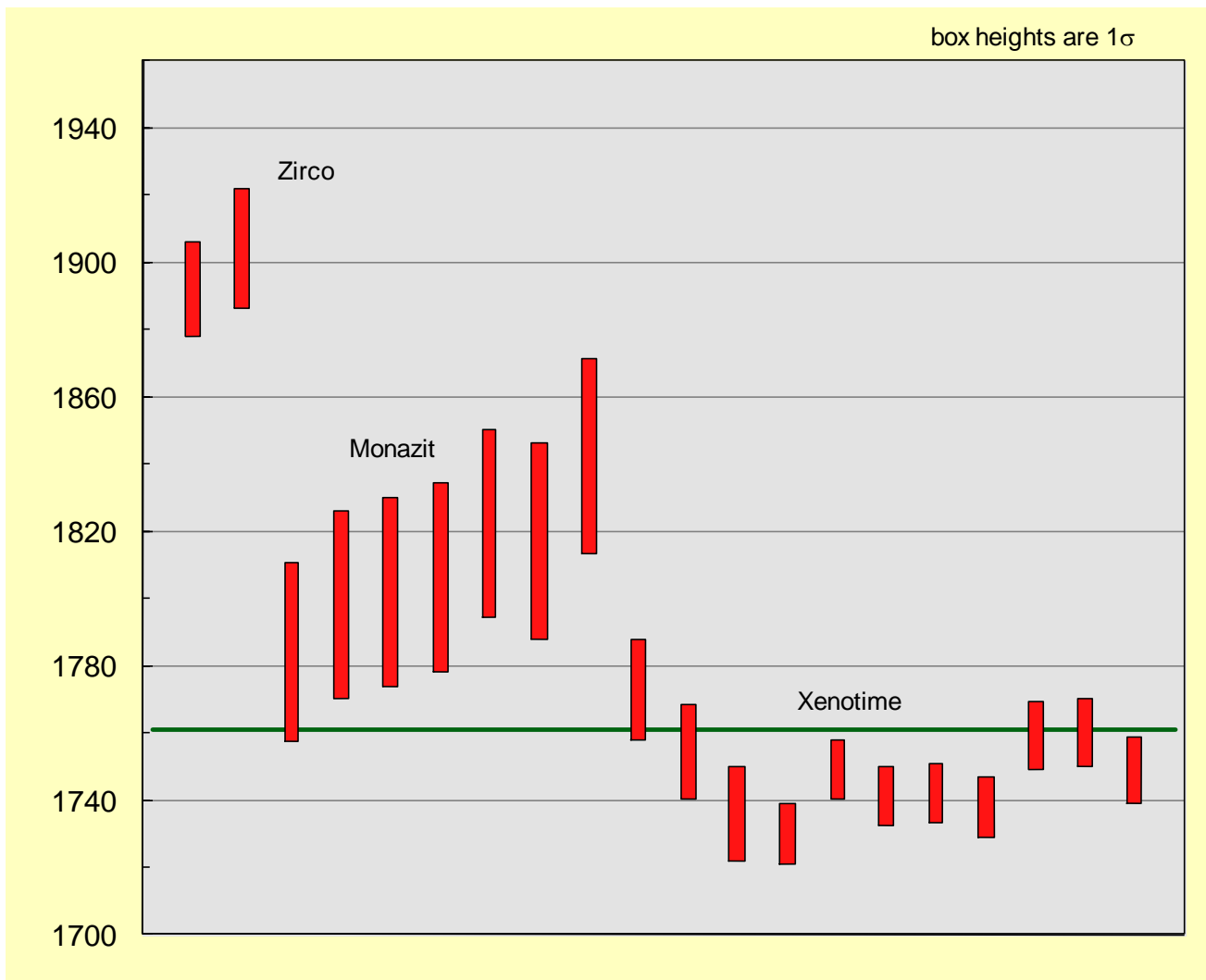
Fig 17. The ages of xenotime are near each other and could be correlated with post-orogenic granites. Zircon is older and near granulite in age.

4   DISCUSSION AND CONCLUSION

Mäkärä's gold-hematite-quartz is strongly weathered and difficult to study. Samples were divided in to three parts for polished thin section study and comminution by selFrag and roller crusher that led to heavy minerals concentrations. Pure gold occur in very small grains from 3 to 5 microns with acicular hematite and hematite-rutile intergrowths, also sulphide minerals mainly chalcopyrite and Cu and Zn bearing silicates and aggregated grains of zircon, monazite and xenotime are observed.

GTK
gtk.fi

The U-Pb dating results indicate that the age of xenotime and monazite in Mäkärä's dyke corresponds well with the age of postorogenic granites such as Nattanen although xenotime is slightly younger. The zircon age of the dyke is little younger than the granulite.

References

Andersen, T., Griffin, W.L., Jackson, S.E., Knudsen, T.-L., Pearson, N.J. (2004) Mid-Proterozoic magmatic arc evolution at the southwest margin of the Baltic Shield. Lithos 73:289–318.

Belousova, E.A., Griffin, W.L. and O'Reilly, S.Y. (2006) Zircon crystal morphology, trace element signatures and Hf isotope composition as a tool for petrogenetic modeling: examples from Eastern Australian granitoids. J Petrol 47:329–353.

Härkönen, Ilkka (1987) Kultatutkimukset Mäkärärovan alueella Sodankylässä vuosina 1980 - 1985. 18 s., 20 liites. *Geologian tutkimuskeskus, arkistoraportti, M19/3724/-87/1/10.*

Hölttä, P., Huhma, H., Mänttäri, I., and Paavola, J. (2000) P-T-t development of Archaean granulites in Varpaisjärvi, central Finland. II. Dating of high-grade metamorphism with the U-Pb and Sm-Nd methods. Lithos 50:121-136.

Huhma, H., Mänttäri, I., Peltonen, P., Kontinen, A., Halkoaho, T., Hanski, E., Hokkanen, T., Hölttä, P., Juopperi, H., Konnunaho, J., Lahaye, Y., Luukkonen., E., Pietikäinen. K., Pulkkinen, A., Sorjonen-Ward, P., Vaasjoki, M. & Whitehouse, M. (2012). The age of the Archaean greenstone belts in Finland. In: Hölttä P. (ed.) The Archaean of the Karelia Province in Finland. Geological Survey of Finland, Special Paper 54, 74−175.

Jackson, S.E., Pearson, N.J., Griffin, W.L., and Belousova E.A. (2004) The application of laser ablation-inductively coupled plasma-mass spectrometry to in-situ U-Pb zircon geochronology. Chem Geol 211:47-69.

Ludwig, K.R. (2003) Isoplot 3.00 A geochronological toolkit for Microsoft Excel. Berkeley Geochronology Center, Berkeley, 70.

Meriläinen, K., 1976. The granulite complex and adjacent rocks in Lapland, northern Finland. Bulletin of the Geological Survey of Finland 281, 1−129.

Müller, W., M. Shelley, Miller, P., and Broude, S. (2009). "Initial performance metrics of a new custom-designed ArF excimer LA-ICPMS system coupled to a two-volume laser-ablation cell. Journal of Analytical Atomic Spectrometry, 24: 209-214.

Pajunen, M. and Poutiainen, M. (1999) Palaeoproterozoic prograde metasomatic-metamorphic overprint zones in Archaean tonalitic gneisses, eastern Finland. Bulletin of the Geological Society of Finland 71, 73-132.

Patchett, J. and Kouvo, O. (1986) Origin of continental crust of 1.9-1.7 Ga age: Nd isotopes and U-Pb zircon ages in the Svecokarelian terrain of south Finland. Contributions to Mineralogy and Petrology 92, 1-12.

Rosa, D.R.N., Finch, A.A., Andersen T., and Inverno C.M.C. (2009) U-Pb geochronology and Hf isotope ratios of magmatic zircons from the Iberian pyrite belt. Miner. Petrol. 95: 47-69.

Sarapää, O. & Sarala, P. (2013) Rare earth element and gold exploration in glaciated terrain - example from the Mäkärä area, northern Finland. Geochemistry: Exploration, Environment, Analysis 13, 131–143.
Stacey, J.S. and Kramers, J.D. (1975). Approximation of Terrestrial Lead Isotope Evolution by a 2-Stage Model. Earth and Planetary Science Letters 26(2): 207-221

Stacey, J.S. and Kramers, J.D. (1975). Approximation of Terrestrial Lead Isotope Evolution by a 2-Stage Model. Earth and Planetary Science Letters 26(2): 207-221

Appendix I

Appendix I

Chemical analyses of drill core samples from R318 using ICP-AES

Tilaajan näytetunnus	Sample wt (kg)	Au µg/kg	As %	Al %	Ba %	Be %	Ca %	Co %	Cr %	Cu %	Fe %	K %	La %	Li %	Mg %
	32	+704P	+720P	+720P	720P	720P	+720P	+720P	+720P	+720P	+720P	+720P	720P	720P	+720P
3724/10															
R318 1.00- 2.20	2,93	233	<0.01	6,31	0,061	<0.001	1,41	0,002	0,012	0,004	7,83	2,18	0,004	0,001	0,88
R318 2.20- 4.20	3,12	175	<0.01	8,76	0,032	<0.001	0,18	<0.001	0,050	0,005	7,72	2,02	0,004	<0.001	0,32
R318 4.20- 5.60	3,37	72	<0.01	7,49	0,026	<0.001	0,04	<0.001	0,085	0,003	7,34	3,39	0,008	<0.001	0,35
R318 5.60- 7.00	2,25	77	<0.01	8,13	0,032	<0.001	0,38	0,002	0,077	0,006	8,06	2,77	0,003	<0.001	0,51
R318 7.00- 8.00	2,60	41	<0.01	5,36	0,013	<0.001	0,08	0,001	0,112	<0.002	15,80	2,08	0,005	<0.001	0,28
R318 8.00- 9.00	2,44	126	<0.01	6,44	0,015	<0.001	0,02	0,001	0,024	0,003	16,20	2,45	0,007	<0.001	0,25
R318 9.00- 9.50	1,46	1790	<0.01	2,99	0,007	<0.001	0,05	<0.001	0,028	0,002	39,40	1,19	0,007	<0.001	0,12
R318 9.50- 11.00	4,18	1840	<0.01	7,05	0,017	<0.001	0,02	0,003	0,064	0,005	13,70	3,47	0,008	<0.001	0,38
R318 11.00- 12.00	3,93	7960	<0.01	3,02	0,010	<0.001	<0.01	<0.001	0,040	<0.002	40,40	1,74	0,007	<0.001	0,15
R318 12.00- 13.00	3,65	762	<0.01	5,04	0,012	<0.001	0,01	0,002	0,019	0,005	25,00	2,61	0,008	<0.001	0,26
R318 13.00- 14.00	2,64	672	<0.01	5,49	0,022	<0.001	<0.01	<0.001	0,013	<0.002	14,90	3,03	0,005	<0.001	0,26
R318 14.00- 19.50	1,28	117	<0.01	5,95	0,030	<0.001	<0.01	<0.001	0,004	<0.002	14,50	3,39	0,005	<0.001	0,31
R318 19.50- 21.20	1,42	159	<0.01	7,18	0,028	<0.001	0,01	<0.001	<0.003	<0.002	6,67	4,22	0,014	<0.001	0,32
R318 21.20- 26.00	0,53	49	<0.01	6,62	0,070	<0.001	0,46	0,001	<0.003	0,008	7,56	2,97	0,004	0,001	0,47

Tilaajan näytetunnus	kapaino kg	Mn %	Mo %	Ni %	P %	Pb %	S %	Sb %	Sc %	Si %	Sr %	Ti %	Y %	V %	Zn %
	32	+720P	+720P	+720P	+720P	+720P	+720P	+720P	720P	720P	720P	+720P	+720P	+720P	+720P
3724/10															
R318 1.00- 2.20	2,93	0,055	<0.005	<0.005	<0.05	<0.01	<0.02	<0.01	<0.002	30,80	0,013	0,39	0,003	0,008	0,006
R318 2.20- 4.20	3,12	0,016	<0.005	0,006	<0.05	<0.01	<0.02	<0.01	0,002	30,00	<0.003	0,74	0,004	0,015	<0.005
R318 4.20- 5.60	3,37	0,013	<0.005	0,010	<0.05	<0.01	<0.02	<0.01	<0.002	32,10	<0.003	0,58	0,005	0,015	<0.005
R318 5.60- 7.00	2,25	0,022	<0.005	0,008	<0.05	<0.01	<0.02	<0.01	0,002	30,10	<0.003	0,69	0,003	0,019	<0.005
R318 7.00- 8.00	2,60	0,011	<0.005	0,008	<0.05	<0.01	<0.02	<0.01	<0.002	28,20	<0.003	0,43	0,003	0,015	<0.005
R318 8.00- 9.00	2,44	0,010	<0.005	0,006	0,06	<0.01	<0.02	<0.01	<0.002	27,70	<0.003	0,50	0,004	0,014	<0.005
R318 9.00- 9.50	1,46	0,010	<0.005	<0.005	0,07	<0.01	<0.02	<0.01	<0.002	16,70	<0.003	0,18	0,005	0,021	0,006
R318 9.50- 11.00	4,18	0,011	<0.005	0,007	0,06	<0.01	<0.02	<0.01	<0.002	26,70	<0.003	0,68	0,005	0,022	<0.005
R318 11.00- 12.00	3,93	0,005	<0.005	<0.005	<0.05	<0.01	<0.02	<0.01	<0.002	16,50	<0.003	0,27	0,005	0,014	0,006
R318 12.00- 13.00	3,65	0,010	<0.005	<0.005	<0.05	<0.01	<0.02	<0.01	<0.002	24,10	<0.003	0,62	0,005	0,019	<0.005
R318 13.00- 14.00	2,64	0,009	<0.005	<0.005	<0.05	<0.01	<0.02	<0.01	<0.002	29,50	<0.003	0,40	0,003	0,009	<0.005
R318 14.00- 19.50	1,28	0,008	<0.005	<0.005	<0.05	<0.01	<0.02	<0.01	0,002	29,00	<0.003	1,13	0,005	0,020	<0.005
R318 19.50- 21.20	1,42	0,008	<0.005	<0.005	<0.05	<0.01	<0.02	<0.01	<0.002	30,70	<0.003	1,15	0,004	0,023	<0.005
R318 21.20- 26.00	0,53	0,092	<0.005	0,006	0,12	<0.01	<0.02	<0.01	0,002	32,60	0,004	0,98	0,005	0,007	0,011